

UNCLASSIFIED

AD **407 918**

DEFENSE DOCUMENTATION CENTER

FOR

SCIENTIFIC AND TECHNICAL INFORMATION

CAMERON STATION, ALEXANDRIA, VIRGINIA



UNCLASSIFIED

NOTICE: When government or other drawings, specifications or other data are used for any purpose other than in connection with a definitely related government procurement operation, the U. S. Government thereby incurs no responsibility, nor any obligation whatsoever; and the fact that the Government may have formulated, furnished, or in any way supplied the said drawings, specifications, or other data is not to be regarded by implication or otherwise as in any manner licensing the holder or any other person or corporation, or conveying any rights or permission to manufacture, use or sell any patented invention that may in any way be related thereto.

A B S T R A C T

Several possible explanations of the mechanism of the break-up of shaped charge jets are suggested. In particular, an approach using the assumption of visco-plastic flow is presented in detail. According to this approach, a constant area jet with linear velocity gradient breaks first at the tip, and then the break-up progresses back towards the rear. The average length of the fragments could be adjusted to two per cent of the original jet length if a coefficient of viscosity of 100 lb.-sec./ft.² were used.

I. INTRODUCTION

This is a progress report on a research project which utilized shaped charge jets as a means to study the properties and behaviors of metals under a very high rate of strain. In connection with the analysis of hypervelocity impacts, Chou^{1,2} and Riney³ have assumed that materials possess a visco-plastic property. At present, the numerical values of the coefficient of viscosity, or the stress-strain rate relations of materials under high rate of strain are not known. There are definite disagreements among different investigators as to the existence and/or significance of viscosity. Experimental evidence apparently is needed.

It is difficult to evaluate the importance of viscosity from most impact experiments because compressibility effects in the form of stress or shock waves is always present. A one-dimensional high-strain-rate tension experiment would be most ideal for this purpose. The jet ejected from a shaped charge approaches this ideal model very closely and, therefore, was chosen for this study. If the jet is assumed to behave as a visco-plastic material and, if a separation criterion similar to the one given in references 1 and 2 is used, it is shown that the break-up of the jet may be predicted and the coefficient of viscosity numerically evaluated.

However, it must be pointed out that according to experiments performed by DiPersio, Simon and Martin⁴, the behavior of the jets obeys the simple Hopkinson's scaling law. If this scaling law is valid, then the viscous, or strain rate, effect must be unimportant. Therefore, it appears that the visco-plastic model probably cannot singly describe the motion of the jet and its break-up mechanism.

Although our original objective, i.e., the numerical determination of the coefficient of viscosity through the use of metal jets, appears unsuccessful, the study of the shaped charge jet was continued in order to obtain a more definite conclusion concerning the applicability of the visco-plastic theory. Understanding of the break-up process is also important if theoretical improvement of the penetration power of the jet is to be achieved.

A statistical approach which is based upon the assumption that the tensile strength for a given material is not exactly constant but shows a scatter characteristic may also be used to describe the jet behavior. This approach was first proposed by Mott in studying the fragmentation of shell cases.

In another approach it is assumed that the jet is at a high temperature immediately after formation and that it is also in a molten state which can be subjected to a very large elongation. As the jet moves forward, it cools and gradually changes into a

solid state which cannot sustain a large magnitude of elongation and thus breaks up.

The last two approaches are currently being investigated.

II. DESCRIPTION OF THE BREAK-UP OF SHAPED CHARGE JETS

The basic theories of the formation of a shaped charge jet and its penetration into targets were first presented by Birkhoff, MacDougall, Pugh and Taylor in 1948⁵. Since that time, these theories have been refined by Eichelberger⁶ and have been verified experimentally by Eichelberger and Pugh^{7,8}. These theories, however, do not attempt an explanation of the break-up mechanism of the jet.

For most jets, the metal mass is uniformly distributed along the axial direction, although, depending on the charge and liner design, it could be variably distributed. The velocity is maximum at the tip and varies linearly to a minimum at the rear. The velocity gradient is constant at a given time, except possibly in the region near the tip. There is usually a slug with a large mass following the main jet and traveling at a low velocity. For the present purpose, the slug will not be considered.

Because of the difference in velocity between the tip and the rear, a condition of constant strain-rate exists, and the jet elongates. For a typical jet the velocity at the tip is approximately 8 km./sec. and at the rear 2 km./sec. This continuous jet eventually breaks up after approximately 120 μ sec. The total elongation may be of the order of 300 to 400% of the original length at the time of its formation. This value of elongation is much higher than the static ultimate elongation of the usual jet metals, i.e., copper or steel. After the break-up, the jet changes to short cylindrical segments with an average length of approximately two one-hundredths of the length of the final continuous jet; in other words, the jet breaks into approximately 50 segments. Following the break up, the length of each segment remains unchanged although the spacings between segments continues to increase due to the difference in velocities.

According to a scaled shaped charge experiment performed at BRL⁴, the Hopkinson's scaling law may be applied to shaped charge jets with respect to the following parameters: velocity gradient, jet diameter, number of particles produced, average particle length, penetration depth and standoff distance. According to this scaling law, if two shaped charges are identical in all but size, with a linear scale factor $\lambda = \frac{L_2}{L_1}$, then the velocity and geometry of the second jet are identical to those of the first one for points located at distances λ times

that of the first one and occurring at a time λ times that of the first one.

The Hopkinson's scaling law was first proposed for the study of the pressure and velocity disturbances due to explosions. Judging from the results of numerous hypervelocity cratering experiments, it is believed that this scaling law is applicable to impact problems. Concerning its application to shaped charge jets, reference 4 appears to be the only source of experimental evidence devoted to the investigation of this problem. It appears that additional tests are needed before a firm statement about the scaling law in shaped charge jets can be made.

III. POSSIBLE MODELS FOR THE BREAK-UP PROCESS

In connection with practical applications, there have been several hypotheses concerning the break-up process. One of these assumes that the jet breaks up simultaneously at a certain time after its formation. Another hypothesis states that the jet breaks one segment at a time and that it occurs when the jet element is at a certain distance from the base of the charge. At the present time, there are not sufficient experimental evidences to verify which of these hypotheses is valid. Furthermore, these hypotheses do not offer any explanation of the break-up mechanism.

In the following discussion, three possible models for the break-up process are suggested and described briefly. They are the visco-plastic model, the failure scatter model, and the molten phase model.

A. Visco-Plastic Model

In this approach, the material of the jet is assumed to follow a simple visco-plastic stress-strain rate relation:

$$\tau = \tau_y + \mu \dot{\epsilon}$$

According to this relation, the stress acting between two adjacent elements in the jet is equal to the yield stress τ_y (a constant for perfectly plastic material), plus a viscous stress depending on the strain rate $\dot{\epsilon}$. Combining this equation with the equation of motion, the governing equation (equation 8) may be derived. This equation, together with the proper boundary and initial conditions, may be solved to give the time history of the motion of the jet.

To predict the break-up, a separation criterion similar to that proposed in reference 1 is used. It postulates that the jet can sustain very large strain and elongation without breaking as long as the viscous stress is larger than a critical value. It will be shown in the next section that by assigning proper values to the

In the following discussion, three possible models for the break-up process are suggested and described briefly. They are the visco-plastic model, the failure scatter model, and the molten phase model.

A. Visco-Plastic Model

In this approach, the material of the jet is assumed to follow a simple visco-plastic stress-strain rate relation:

$$\tau = \tau_y + \mu \dot{\epsilon}$$

According to this relation, the stress acting between two adjacent elements in the jet is equal to the yield stress τ_y (a constant for perfectly plastic material), plus a viscous stress depending on the strain rate $\dot{\epsilon}$. Combining this equation with the equation of motion, the governing equation (equation 8) may be derived. This equation, together with the proper boundary and initial conditions, may be solved to give the time history of the motion of the jet.

To predict the break-up, a separation criterion similar to that proposed in reference 1 is used. It postulates that the jet can sustain very large strain and elongation without breaking as long as the viscous stress is larger than a critical value. It will be shown in the next section that by assigning proper values to the

coefficient of viscosity, the jet may be made to break-up from the tip, one segment after another, with an average length of two per cent of the total jet length.

Although this approach could explain the process, it is doubtful that it definitely represents the true phenomenon. The objection to the visco-plastic assumption is that the Hopkinson's scaling law excludes any strain rate effect. In other words, if a jet follows the Hopkinson's scaling law, the viscous effect must be unimportant.

B. The "Failure-Scatter" Model

This approach was first suggested by N. F. Mott⁹ in 1947 for the study of fragmentation of shell cases. It is based on the assumption that there exists a scatter in the value of the reduction in area (or value of strain) at which fracture occurs in a tensile test.

This theory may easily be applied to the shaped charge jet. If there were no scatter (the strain at fracture was perfectly definite), the stretching jet would break at all points simultaneously. If scatter in strain exists, there is, in any length of the jet, a finite probability of fracture which increases rapidly as the strains approach the critical value. Then fracture will first occur at one point. After fracture, the free surface can not sustain stress, and

a release stress wave will propagate inward. The unstressed (and unstrained) regions spread with a velocity which can be calculated by either the elastic, plastic-rigid, or visco-plastic assumptions. This is shown in figure A in which a fracture is assumed to have occurred at A and the stress has been released in the shaded regions AB and A'B':

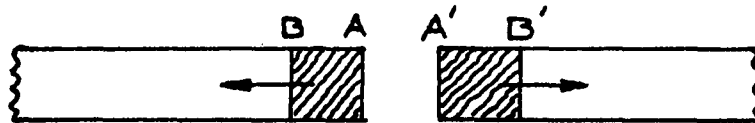


Figure A

Fracture can no longer occur in the shaded regions because the material in this region is rigid, and no stretching occurs. In the unshaded regions, plastic flow and stretching will continue. Strain increases and fracture becomes more likely. The average size of the fractured segments will be determined by the rate at which the shaded regions in figure A propagate, thereby preventing further fractures. Segment size also depends upon the scatter property which may be expressed as the probability, P , that the tensile test specimen breaks before a strain, ϵ , is reached.

$$P = P(\epsilon)$$

a release stress wave will propagate inward. The unstressed (and unstrained) regions spread with a velocity which can be calculated by either the elastic, plastic-rigid, or visco-plastic assumptions. This is shown in figure A in which a fracture is assumed to have occurred at A and the stress has been released in the shaded regions AB and A'B':

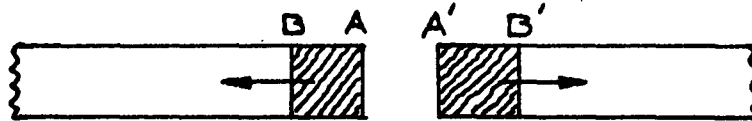


Figure A

Fracture can no longer occur in the shaded regions because the material in this region is rigid, and no stretching occurs. In the unshaded regions, plastic flow and stretching will continue. Strain increases and fracture becomes more likely. The average size of the fractured segments will be determined by the rate at which the shaded regions in figure A propagate, thereby preventing further fractures. Segment size also depends upon the scatter property which may be expressed as the probability, P , that the tensile test specimen breaks before a strain, ϵ , is reached.

$$P = P(\epsilon)$$

This probability, which must be determined from experiments, is not known at present.

This theory gives no explanation of the fact that the jet can elongate to a length three or four times longer than its original length.

C. The Molten State Model

Statically, a metal can not sustain an elongation of more than 100%. Two factors may contribute to the 300 to 400% elongation of the jet; namely, strain rate and temperature. If the strain rate effect is rejected as a possibility, the high temperature explanation seems most reasonable.

Immediately after formation, the temperature of the slug is estimated to be above 1000°C in the center and somewhat cooler near the surface¹⁰. The temperature in the jet is also believed to be very high. An estimation by Pugh* indicates that the slug temperature is just below the melting point of the metal. At these high temperatures, the metal can easily elongate to four or five times its original length without breaking. As the jet moves forward, it cools due to radiation and air convection. As the temperature decreases, the metal changes into the solid state and can no longer sustain large elongation.

*Private Communication

The true mechanism of the break-up process is probably more involved than that indicated by any one of these simplified models. At the present time, the heat transfer property of the jet is under investigation and, it is hoped, the validity of the molten state model can be determined approximately. The results of the visco-plastic flow analysis are presented in the next section for future reference.

IV. EQUATIONS, CRITERIA, AND SOLUTIONS OF THE VISCO-PLASTIC MODEL

A. The Governing Equations

The equations in this section are derived for a jet with variable cross-section area. The analysis for the constant area jet will be treated as a particular case of the former. Further, LaGrange coordinates are to be assumed for the determination of these equations.

The continuity equation for the jet is:

$$\rho_0 A_0 dx = \rho A d\bar{x} \quad (1)$$

or,

$$\frac{\rho_0 A_0}{\rho A} = \frac{d\bar{x}}{dx} = 1 + \epsilon \quad (2)$$

The stress-strain relation is assumed to be viscoplastic, which for simple tension has the following form:

$$\sigma = \sigma_y + \mu \dot{\epsilon} \quad (3)$$

Referring to figure B, the equation of motion may be shown to be:

$$\rho A d\bar{x} \frac{\partial v}{\partial t} - \sigma \frac{dA}{d\bar{x}} d\bar{x} - A \frac{\partial \sigma}{\partial \bar{x}} d\bar{x} = 0 \quad (4)$$

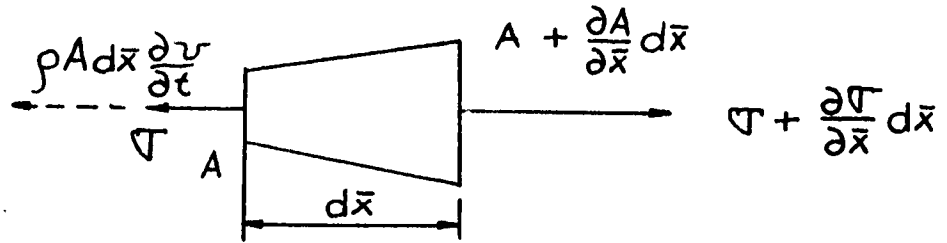


Figure B

Introducing equations 1 and 2 in equation 4 yields:

$$\rho A \frac{\partial v}{\partial t} - \sigma \frac{dA}{d\bar{x}} - A \frac{\partial \sigma}{\partial \bar{x}} = 0 \quad (5)$$

Substituting equation 3 into equation 5 yields:*

$$\frac{\partial v}{\partial t} - \frac{\mu}{\rho_0} \frac{\partial^2 v}{\partial x^2} - \frac{1}{A_0} \frac{dA_0}{dx} \cdot \frac{\mu}{\rho_0} \frac{\partial v}{\partial x} - \frac{1}{A_0} \frac{dA_0}{dx} \cdot \frac{\sigma_0}{\rho_0} = 0 \quad (6)$$

Introducing the following dimensionless quantities:

$$x' = \frac{x}{l}; \quad v' = \frac{v}{V_0}; \quad t' = \frac{t V_0}{l}; \quad R = \frac{l V_0}{\mu}; \quad B = \frac{\sigma_y l}{\mu V_0} \quad (7)$$

* In the second term of the left hand side, a factor $\frac{A}{A_0}$ has been neglected.

Equation 6 becomes:

$$R \frac{\partial v'}{\partial t'} - \frac{\partial^2 v'}{\partial x'^2} - \frac{dA_0}{A_0 dx'} \cdot \frac{\partial v'}{\partial x'} - B \frac{dA_0}{A_0 dx'} = 0 \quad (8)$$

This is the governing differential equation for the velocity v' in which t' and x' represent the independent variables. If the boundary condition and initial conditions are simple, this equation may be solved by Laplace transform techniques, separation of variables or other standard methods. For complicated initial and boundary conditions, a finite difference method must be used.

B. The Constant Area Jet

In the problem of a constant area shaped charge jet the governing differential equation of motion will be a particular case of equation 8 obtained by substituting $\frac{dA_0}{dx'} = 0$, thus:

$$R \frac{\partial v'}{\partial t'} - \frac{\partial^2 v'}{\partial x'^2} = 0 \quad (9)$$

Since this analysis is directed to the determination of the difference in velocities, the jet is assumed to have zero velocity at the tail end, maximum initial velocity V_0 at the tip and linear velocity variation at all intermediate points. At the tip and the tail, stress-free end conditions are assumed. From equation 3, the end

conditions are $\frac{\partial v'}{\partial x'} = \frac{-\sigma_0}{\mu}$ at $\begin{cases} x' = 0 \\ x' = 1 \end{cases}$. For the present

problem which involves very high strain-rate, $\frac{\sigma_0}{\mu}$ is small compared with the average strain rate, and it will therefore be neglected. The initial and boundary conditions are:

$$\begin{aligned} v' &= x' & \text{at } t' = 0 ; 0 < x' < 1 \\ \frac{\partial v'}{\partial x'} &= 0 & \text{at } t' > 0 ; x' = 0 ; x' = 1 \end{aligned} \quad (10)$$

Solution of the constant area jet as defined by equations 9 and 10 is obtained by the use of Laplace transformations, as shown in Appendix A.

The velocity, v' , strain ϵ and strain-rate $\frac{\partial v'}{\partial x'}$ are given by equations A-9, A-10, and A-11 respectively in terms of t' and x' .

C. Constant Area Jet (Finite Difference Method)

In order to establish the accuracy of the finite difference method, it was first applied to the constant area jet as defined by equations 9 and 10. Details of the solution are shown in Appendix B. Table 1 and figure 1 show the comparison between the final results obtained from the finite difference method and the LaPlace transformation. The general agreement between these two methods seems satisfactory.

D. Separation Criterion

To determine when break-up or separation occurs a criterion is hypothesized as follows: for jets under a high rate of strain, separation occurs when the following two conditions are simultaneously satisfied:

1. The strain-rate is lower than a critical value; and,
2. The strain is higher than a critical value.

Thus, separation occurs when:

$$\mu \frac{\partial \epsilon'}{\partial x'} < C_1 \sigma_0 ; \quad \epsilon > C_2 \quad (11)$$

where C_1 and C_2 are constants, σ_0 the static ultimate stress. The constant C_2 is assumed to be the static ultimate strain of the material.

E. Numerical Calculations Using Separation Criterion

The values of the various constants must be known before numerical calculations can be performed. Unfortunately, the values of the majority of these constants are not known. To demonstrate the applicability of the theory, all unknown values were estimated.

The constitutive equation 3 contains two constants, the yield stress in pure tension σ_y and the coefficient of viscosity in pure tension μ . It can be shown that if the general visco-plastic relation as proposed by Hohenemser and Prager¹¹ is used, these constants for simple tension may be related to those in pure shear, or

$$\begin{aligned}\sigma &= \sigma_y + \mu \dot{\epsilon} \\ &= \sqrt{3} k + 3 \mu_{\text{SHEAR}} \dot{\epsilon}\end{aligned}$$

where k is the yield stress in shear and μ_{shear} the coefficient of viscosity in shear.

In reference 1, a value of 100 lb.-sec./ft.² is used for μ_{shear} . Hence a μ of 300 lb.-sec./ft.² was adopted for the numerical calculation. From experimental data, the relative velocity between the tip and tail is approximately 6 km./sec.,

therefore, the V_0 was chosen to be 20,000 ft./sec. and the rear end was assumed to be stationary. Further, representable basic values for the various physical properties were assumed to be those of copper. The quantities assigned to $\sigma_0, C_2, \sigma_y^*$ were 30,000 psi, 0.20, and 30,000 psi respectively.

Since all values have been stipulated, the separation criterion states that for a strain-rate $\frac{\partial v'}{\partial x'}$, lower than .7 and ϵ greater than .2, separation occurs. The strain and strain-rate curves for various values of t' are plotted and are shown in figures 2 and 3 respectively. Also shown, as horizontal lines, on these figures is the respective separation criterion for each phase. The intersection of the ϵ_{CR} line and the strain curves yields three points, and these points are plotted in figure 4 as t' versus x' for $\epsilon_{CR} = .2$. Similarly, the strain-rate curves have five points of intersection with the $\left(\frac{\partial v'}{\partial x'}\right)_{CR}$ line, and these are plotted in figure 4 as t' versus x' for $\left(\frac{\partial v'}{\partial x'}\right)_{CR} = 0.7$. The intersection of the critical strain and critical strain-rate curves then determines the t' and x' of separation for the particular physical properties previously outlined. These values are $t'_{CR} = .23$ or $t_{CR} = 11.5 \text{ sec.}$ and $x'_{CR} = .02$ or $x_{CR} = .02 \text{ ft.}$

The fact that $x_{CR} = 0.02 \text{ ft.}$ agrees with the experimental results that the jet breaks into fifty segments. Due

*This value should be approximately 15,000 psi, however, this does not effect the final calculations.
The original jet length l is assumed to be one foot.

to its symmetry, the behavior of the jet at the rear end is identical to that at the tip; therefore, a segment of length 0.02 ft. will simultaneously break off from the rear.

F. Constant Area Jet after Break-up (Finite Difference Method)

From the previous section, it was found that the jet breaks at a distance $x' = .02$ from the tip according to the separation criterion. After the break-up of the tip, the remainder of the jet would behave in a manner similar to the first part, and the second break-up would take place at $x' = .04$. The differential equation, initial and boundary conditions and solution for the second break-up are given in Appendix C and Table 3.

In a similar manner, other break-ups would take place at $x' = .06, .08, .10, \dots$, etc.

The break-up of the first part can be explained by the above hypothesized "separation criterion". But the break-up of the second part cannot be explained using the same criterion, since the true strain in this case always remains above the critical value (see figure 5). However, if the strain is referred to the length after each break-up and not to the original length, then the same criterion will yield the desired results. Hence, this criterion can explain the progress of all the break-ups provided relative lengths are used in the analysis.

G. Variable Area Jet (Finite Difference Method)

It is shown in the preceding section, that for a constant area jet, the break-up initially occurs at the tip and rear ends. If the area of the jet is not constant, i.e., it has a slight fluctuation along the axial direction, then the jet could break at a position which is close to the minimum area section.

For simplicity, the area distribution between $x' = 0$ and $x' = .024$ is assumed to be

$$A_0 = a_0 e^{\lambda \cdot x}$$
$$\frac{dA}{dx} = a_0 \lambda e^{\lambda \cdot x} = A_0 \lambda \quad (12)$$

and for $x' > .024$, A_0 constant = $a_0 e^{.024 \lambda}$ The area distribution, the initial condition and the motion of the jet are assumed to be symmetrical with respect to $x' = 0$. The end condition is then $v' = 0$ at $x' = 0$. The governing equation, equation 6, becomes, for $t' \geq 0$ and $x' \geq 0$

$$\frac{\partial^2 v'}{\partial x'^2} + \lambda \frac{\partial v'}{\partial x'} + B \lambda = R \frac{\partial v'}{\partial t'} \quad (13)$$

The corresponding initial and boundary conditions are:

$$v' = x' \quad \text{at } t' = 0 \quad \text{and } x' \geq 0$$
$$v' = 0 \quad \text{at } x' = 0 \quad \text{and } t' \geq 0 \quad (14)$$

This problem is solved by the finite difference method, and its solution is shown in Appendix D. The results are also presented in figures 6 and 7 in the form of v' vs x' and $\frac{\partial v'}{\partial x'}$ vs x' curves

respectively. It can be seen from figure 6 that in a small neighborhood adjacent to $x' = 0$, the strain-rate $\frac{\partial v'}{\partial x'}$, decreases with respect to time. Since the strain $\frac{\partial u'}{\partial x'}$ increases monotonously, according to the separation criterion, when $\frac{\partial v'}{\partial x'}$ decreases to a critical value, break-up could occur at a position adjacent to the minimum area section.

V. CONCLUDING REMARKS

The detailed solution of the visco-plastic model is presented in this report, although, it may not describe exactly the mechanism of the jet break-up. The other two models are discussed only briefly, and they are currently under investigation. It is quite possible that a combination of these simple models could eventually give the exact description of the jet break-up.

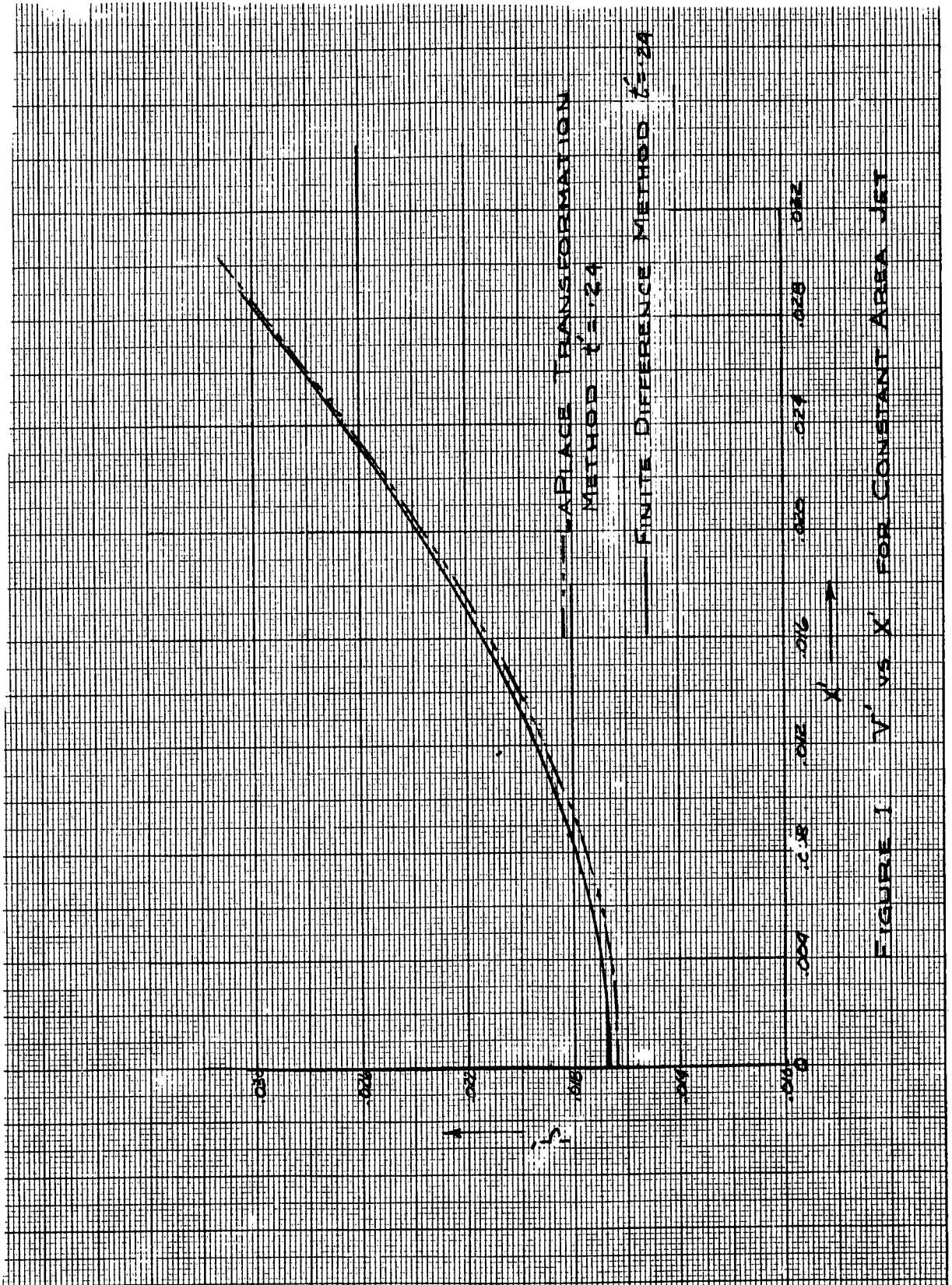
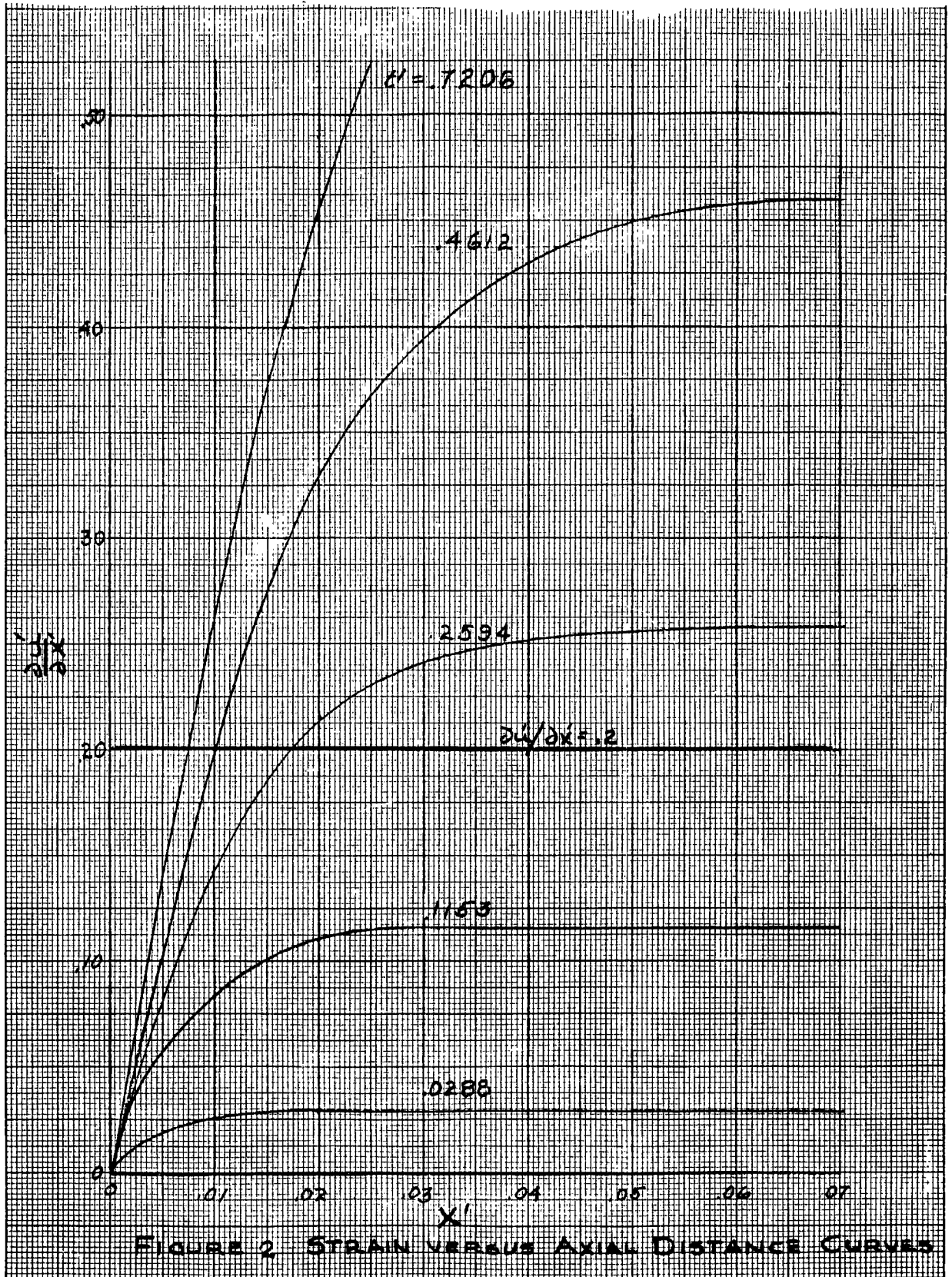


FIGURE 1 V' vs X FOR CONSTANT AREA JET



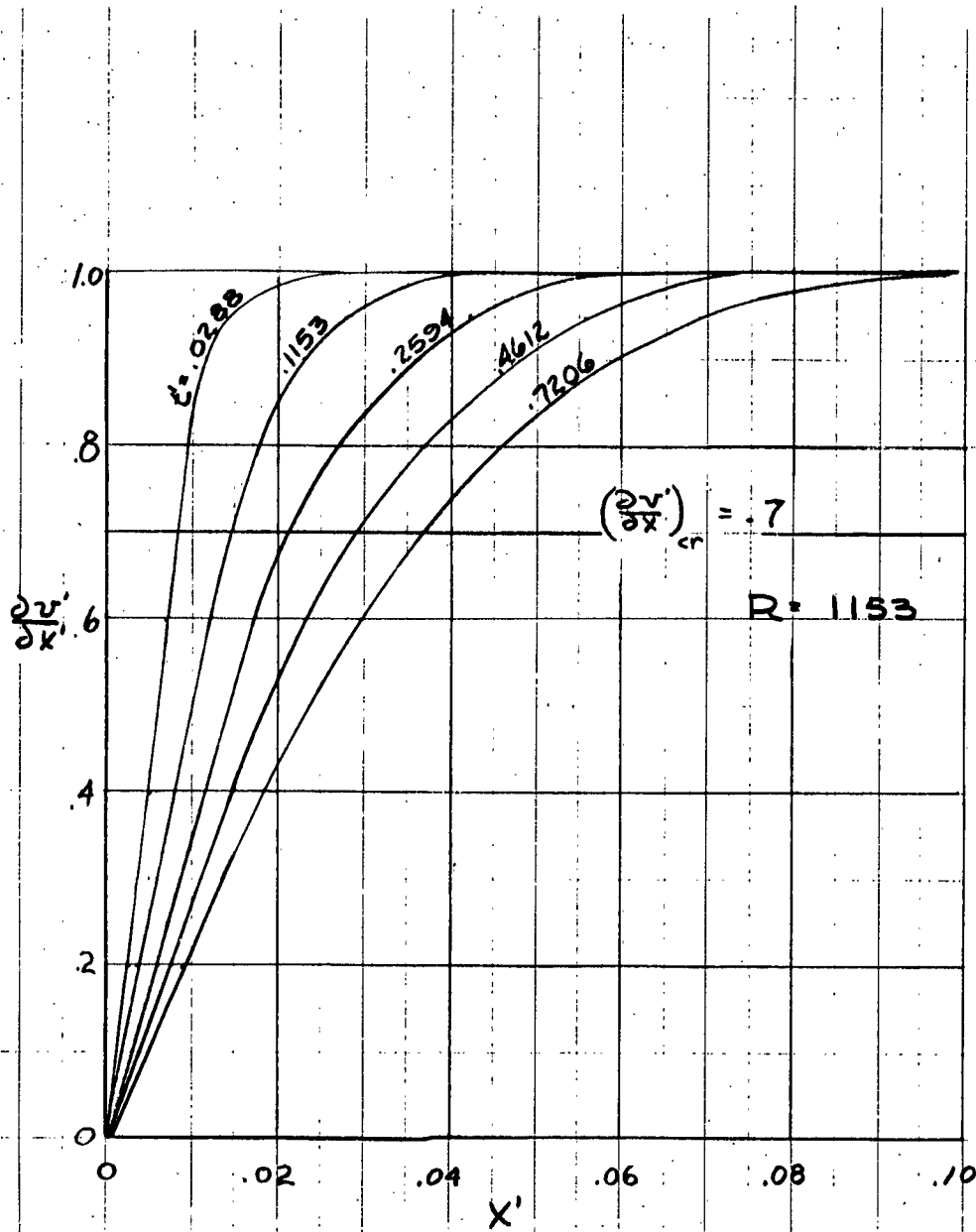


FIGURE 3. STRAIN RATE VS AXIAL DISTANCE CURVES

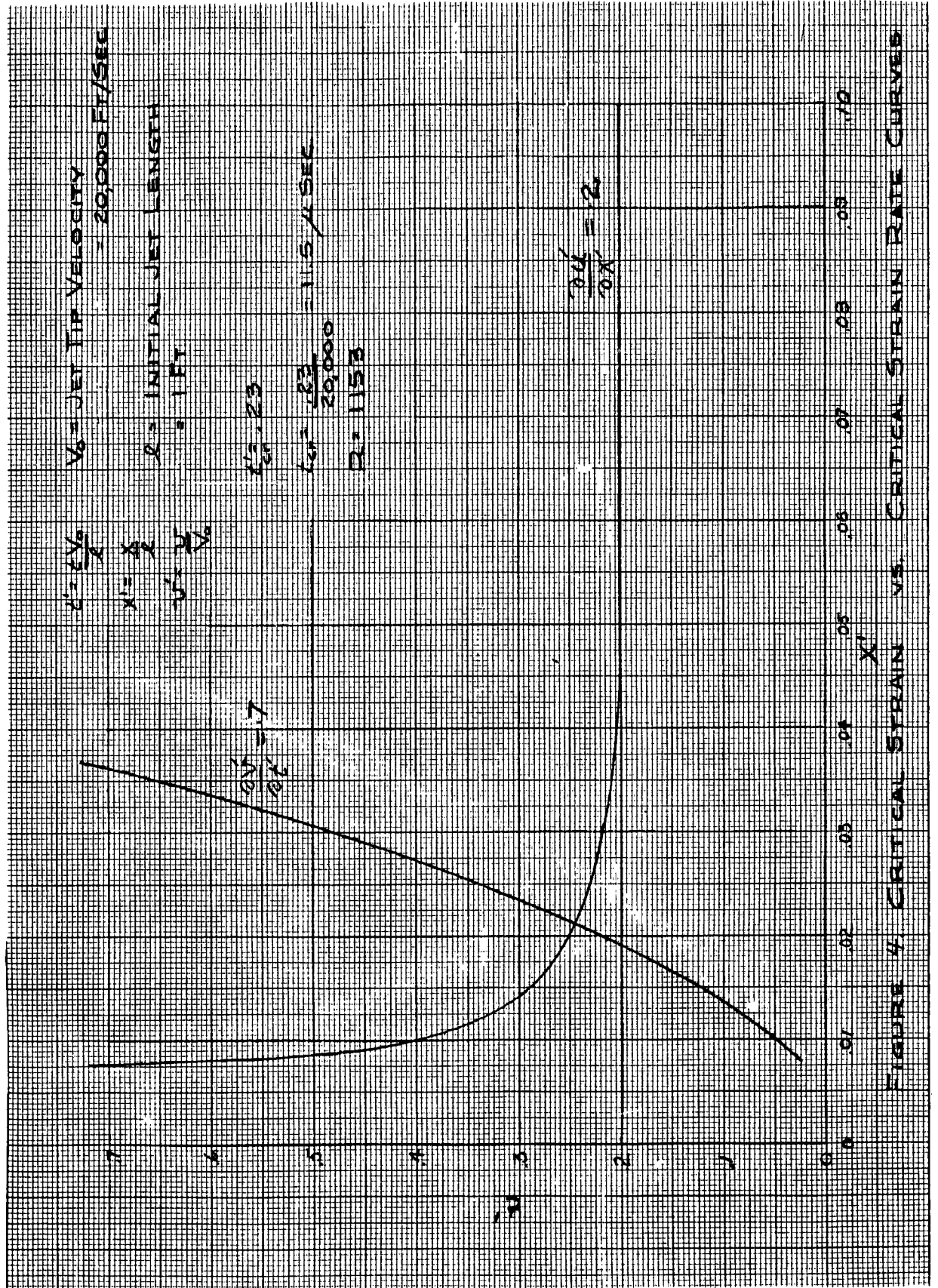


FIGURE 4. CRITICAL STRAIN VS. CRITICAL STRAIN RATE CURVES

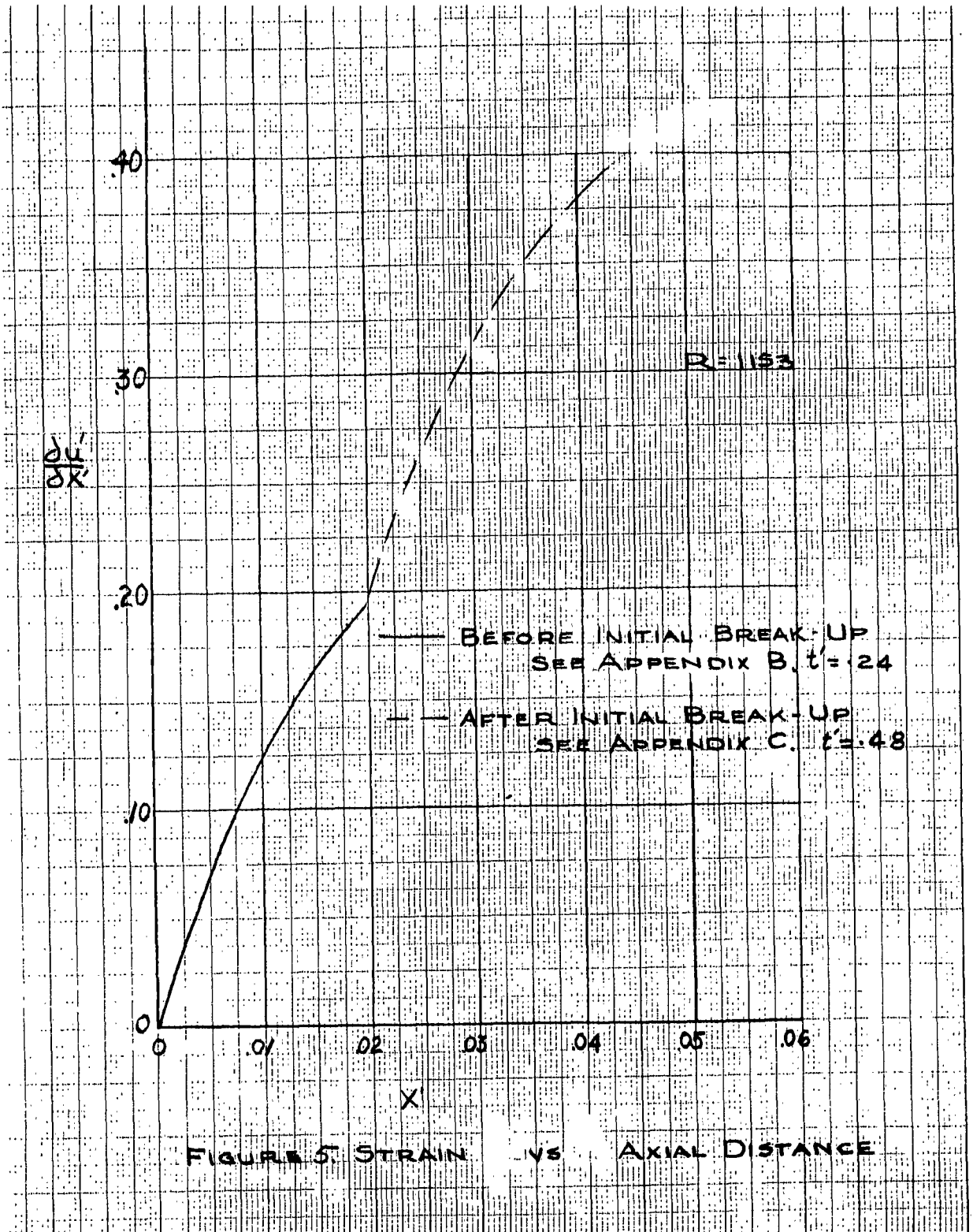


FIGURE 5. STRAIN VS AXIAL DISTANCE

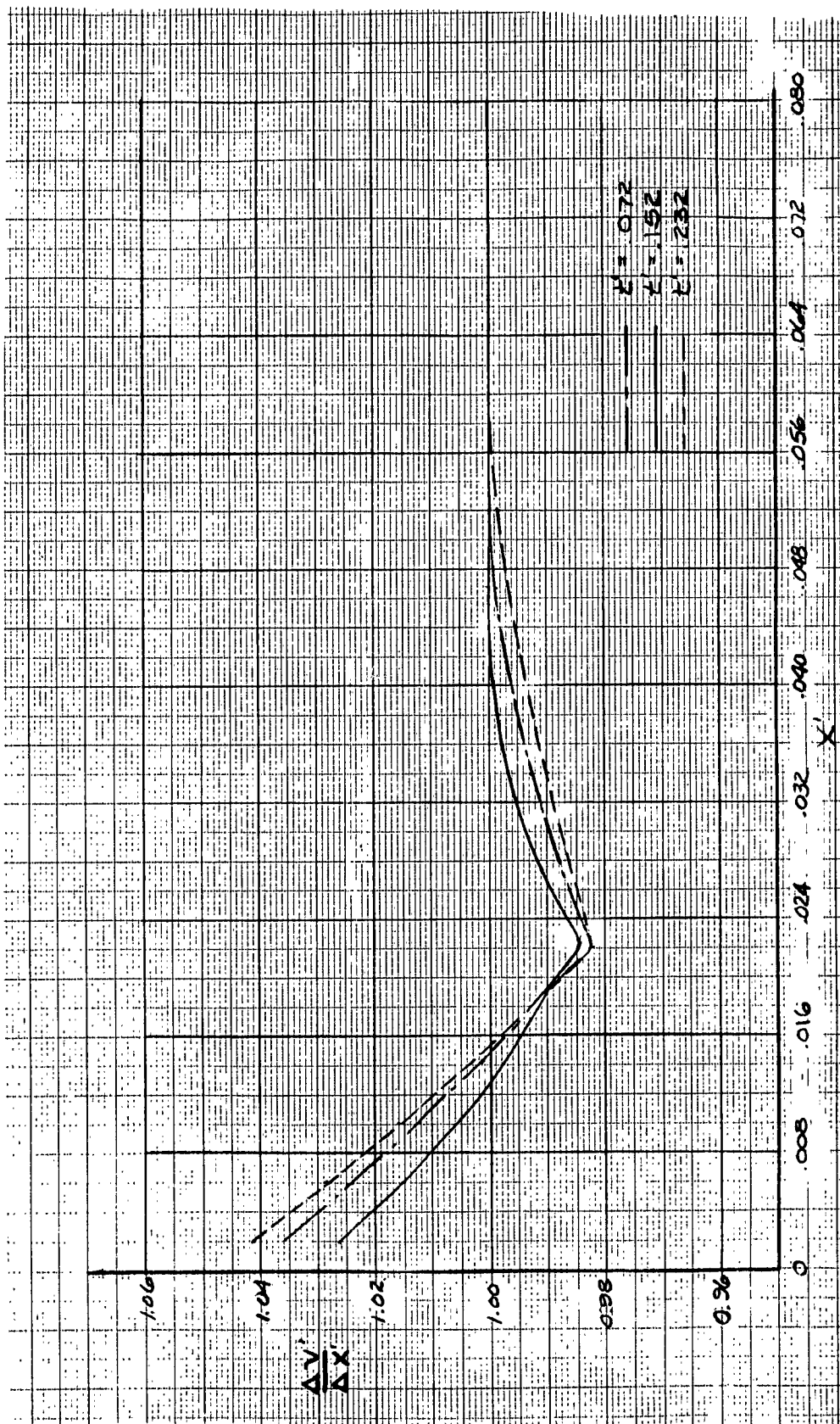


FIGURE 6 $\frac{\Delta V}{\Delta X}$ vs X' FOR VARIABLE AREA JET
(THE AREA BECOMES CONSTANT AT $X' = 0.024$)

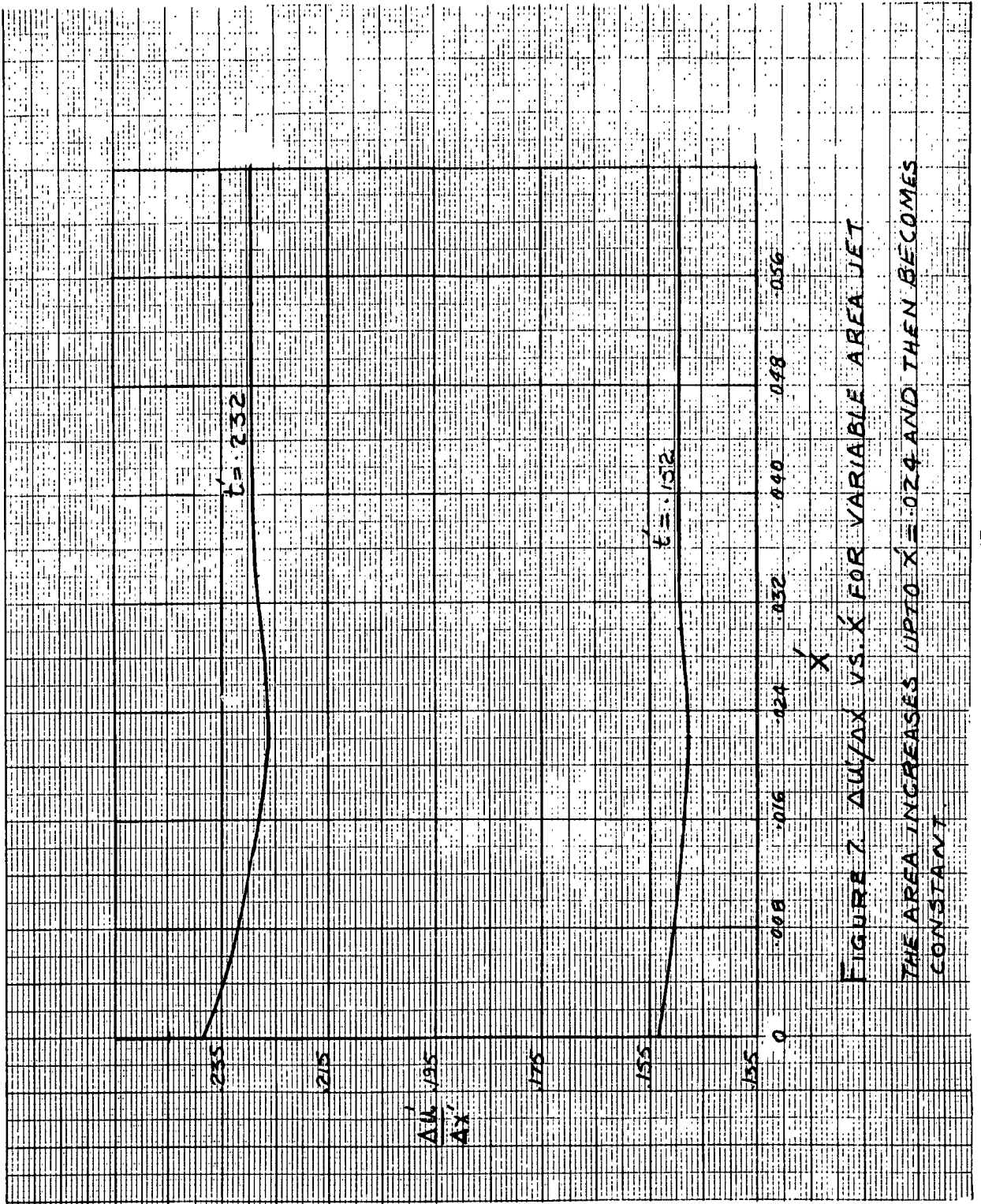


FIGURE 7. $\Delta u / \Delta x$ VS. $\Delta u / \Delta x$ FOR VARIABLE AREA JET
THE AREA INCREASES UP TO $\Delta u / \Delta x = 0.24$ AND THEN BECOMES
CONSTANT.

$H = .00589$ x'	0H	1H	2H	3H	4H	5H
v' by LaPlace Transformation Method	.0163	.0170	.0188	.0220	.0261	.0308
v' by Finite- Difference Method	.0166	.0172	.0191	.0222	.0261	.0308

TABLE 1 - COMPARISON OF SOLUTIONS
OF EQUATION 9 BY LAPLACE TRANSFORMATION
AND
BY FINITE-DIFFERENCE METHOD AT $t' = .24$

t'	$x' = -1H$	$x' = 0$	$x' = 1H$	$x' = 2H$	$x' = 3H$	$x' = 4H$	$x' = 5H$	$x' = 6H$	$x' = 7H$
0	1H	.5H	1H	2H	3H	4H	5H	6H	7H
L	1.25H	1H	1.25H	2H	3H	4H	5H	6H	7H
2L	1.5H	1.25H	1.5H	2.125H	3H	4H	5H	6H	7H
3L	1.6875H	1.5H	1.6875H	2.25H	3.0625H	4H	5H	6H	7H
4L	1.875H	1.6875H	1.875H	2.375H	3.125H	4.03125H	5H	6H	7H
				*	*	*	*	*	*
12L	2.93262H	2.81982H	2.93262H	3.25488H	3.77052H	4.44324H	5.23682H	6.11768H	7.05224H

TABLE 2 - FUNCTION VALUES (v') FROM EQUATION 9
($H = .00589$, $L = .02$)

t'	$x' = -1H$	$x' = 0H$	$x' = 1H$	$x' = 2H$	$x' = 3H$	$x' = 4H$	$x' = 5H$
0L	.02780	.02570	.0278	.0328	.0382	.04375	.04955
1L	.02925	.02780	.02925	.0330	.03828	.04388	.04955
2L	.03040	.02925	.03040	.03376	.03844	.04391	.04963
3L	.03151	.03040	.03151	.03442	.03884	.04404	.04965
				* * * * *	* * * * *		
12L	.03826	.03767	.03826	.04011	.04298	.04680	.05132

TABLE 3 - VALUES OF v' FROM EQUATION 9
 WITH
 INITIAL AND BOUNDARY CONDITIONS AS IN APPENDIX C
 ($H = .00589, L = .02$)

t'	x' = 0	x' = .004	x' = .008	x' = .012	x' = .016	x' = .020	x' = .024	x' = .028
0	0	.004	.008	.012	.016	.020	.024	.028
1L	0	.004028	.008028	.01203	.01603	.02003	.02400	.02800
2L	0	.004041	.008055	.01206	.01605	.02004	.02401	.02800
3L	0	.004055	.008075	.01208	.01608	.02006	.02402	.02801
4L	0	.004066	.008096	.01210	.01610	.02008	.02403	.02801
5L	0	.004076	.008112	.01213	.01612	.02009	.02404	.02802
				* * * * *	* * * * *			
29L	0	.004163	.008273	.01233	.01635	.02032	.02425	.02818

TABLE 4 - FUNCTIONAL VALUES (v')
FOR
THE VARIABLE AREA JET FROM EQUATIONS D-2 AND D-3

(L = .008)

t'	x' = 0	x' = .004	x' = .008	x' = .012	x' = .016	x' = .020	x' = .024	x' = .028
0	0	.004	.008	.012	.016	.020	.024	.028
1L	0	.004028	.008028	.01203	.01603	.02003	.02400	.02800
2L	0	.004041	.008055	.01206	.01605	.02004	.02401	.02800
3L	0	.004055	.008075	.01208	.01608	.02006	.02402	.02801
4L	0	.004066	.008096	.01210	.01610	.02008	.02403	.02801
5L	0	.004076	.008112	.01213	.01612	.02009	.02404	.02802
				* * * * *	* * * * *			
29L	0	.004163	.008273	.01233	.01635	.02032	.02425	.02818

TABLE 4 - FUNCTIONAL VALUES (v')
 FOR
 THE VARIABLE AREA JET FROM EQUATIONS D-2 AND D-3
 (L = .008)

VII. REFERENCES

1. Chou, P. C., "Perforation of Plates by High-Speed Projectiles", *Developments in Mechanics*, Vol. 1, Plenum Press, pp. 286-295, 1951.
2. Chou, P. C., "Visco-Plastic Flow Theory in Hypervelocity Perforation of Plates", *Proceedings of the Fifth Symposium on Hypervelocity Impact*, Vol. 1, part 1, pp. 307-28, April, 1962.
3. Riney, T. D. and Chernoff, P. R., "Inertial, Viscous, and Plastic Effects in High Speed Impact", *Proceedings of the Fifth Symposium on Hypervelocity Impact*, Vol. 1, part 1, pp. 135-162, April, 1962.
4. DiPersio, R., Simon, J., and Martin, T. M., "A study of Jets from Scaled Conical Shaped Charge Liners", *Ballistic Research Laboratories Memorandum Report No. 1298*, August, 1960.
5. Birkhoff, G., MacDougall, D. P., Pugh, E. M., Taylor, G., "Explosives with Lined Cavities", *Journal of Applied Physics*, Vol. 19, No. 6, pp. 563-582, June 1948.
6. Eichelberger, R. J., "Re-Examination of the Nonsteady Theory of Jet Formation by Lined Cavity Charges", *Journal of Applied Physics*, Vol. 26, No. 4, April 1955.
7. Eichelberger, R. J. and Pugh, E. M., "Experimental Verification of the Theory of Jet Formation by Charges with Lined Conical Cavities", *Journal of Applied Physics*, Vol. 23, No. 5, May 1952.
8. Eichelberger, R. J., "Experimental Test of the Theory of Penetration by Metallic Jets", *Journal of Applied Physics*, Vol. 27, No. 1, Jan., 1956.
9. Mott, N. F., "Fragmentation of Shell Cases", *Proceedings, Royal Society (London)*, Vol. 189A, 1947.
10. Cook, Melvin A., "The Science of High Explosives", *ACS Monograph No. 139*, Reinhold, pp. 247-250, 1958.
11. Prager, William, "Introduction to Mechanics of Continua", *Ginn & Co.*, pp. 136-138, 1961.
12. Collatz, L., "The Numerical Treatment of Differential Equations", 3rd Edition, *Springer-Verlag, Berlin, Göttingen, Heidelberg*, 1959.
13. Price, P. H. and Slack, M. R., "Stability and Accuracy of Numerical Solutions of the Heat Flow Equation", *Brit. Journal of Applied Physics*, Vol. 3, pp. 379-384, 1952.

VIII. NOTATIONS

α_0 = original area at $x' = 0$

A_0 = original area =

B = Bingham Number = $\frac{\sigma_v l}{\mu V_0}$

C = Constant

H = Interval length in x' direction

l = Original length of jet

L = Interval length (time direction)

R = Reynold's Number

t = Time

t' = Dimensionless time = $\frac{t V_0}{l}$

u' = Dimensionless displacement

v = Velocity = $\frac{\partial \bar{x}}{\partial t}$

v' = Dimensionless velocity = $\frac{v}{V_0}$

V_0 = Initial jet tip velocity

X = Original abscissa, measured from the end of string in LaGrange coordinates

\bar{x} = Axial fixed coordinate

ϵ = Normal Strain = $\frac{\partial u'}{\partial x'} = \frac{\partial \bar{x}}{\partial X} - 1$

λ = Arbitrary constant of area variation

μ = Coefficient of viscosity in tension

σ = Engineering normal stress = $\frac{\text{Force}}{\text{Original Area}}$

σ_0 = Static ultimate Strength in Tension

σ_y = Yield Strength in Tension

ρ = Density (Mass/Volume)

ρ_0 = Original Density

$\frac{\partial v'}{\partial x'}$ = Dimensionless Strain-rate

IX. APPENDIX A

A. Solutions for the Constant Area Jet

Applying the LaPlace transforms to equation 9 yields

$$L \left\{ R \frac{\partial v'}{\partial t'} \right\} - L \left\{ \frac{\partial^2 v'}{\partial x'^2} \right\} = 0 \quad (A-1)$$

with

$$\bar{v} \equiv L \left\{ v' \right\} \equiv \int_0^{\infty} e^{-pt} dt$$

The transformed differential equation 9 becomes:

$$\frac{d^2 \bar{v}}{dx^2} - R_p \bar{v} = -R x' \quad (A-2)$$

and the transformed boundary conditions are:

$$\frac{d\bar{v}}{dx} = 0 \quad \text{at} \quad t > 0 \quad \text{and} \quad x' = 0, x' = 1 \quad (A-3)$$

The complementary solution of equation A-2 is:

$$\bar{v}_c = c_1 e^{\sqrt{R_p} x'} + c_2 e^{-\sqrt{R_p} x'} \quad (A-4)$$

and the particular solution is:

$$\bar{v}_p = \frac{x'}{p}$$

hence, the general solution of the transformed governing equation

A-2 is:

$$\bar{v} = \frac{x'}{p} + c_1 e^{\sqrt{R_p} x'} + c_2 e^{-\sqrt{R_p} x'} \quad (A-5)$$

Using the boundary conditions, equation A-3, the constants are:

$$C_1 = \frac{(e^{-\sqrt{R_p}} - 1)}{p\sqrt{R_p}(e^{\sqrt{R_p}} - e^{-\sqrt{R_p}})} \quad \& \quad C_2 = \frac{(e^{\sqrt{R_p}} - 1)}{p\sqrt{R_p}(e^{\sqrt{R_p}} - e^{-\sqrt{R_p}})} \quad (A-6)$$

therefore, the solution of equation A-2 after rearranging is:

$$\bar{v} = \frac{1}{p} \left\{ x' + \frac{e^{\sqrt{R_p}(x'-2)} - e^{\sqrt{R_p}(x'-1)} - e^{\sqrt{R_p}(x'+1)} + e^{-\sqrt{R_p}x'}}{\sqrt{R_p}(1 - e^{-2\sqrt{R_p}})} \right\} \quad (A-7)$$

Applying the binomial expansion to the denominator in equation A-7 and realizing that:

$$\frac{1}{1 - e^{-2\sqrt{R_p}}} \cong \sum_{m=0}^{\infty} e^{(-2\sqrt{R_p})m}$$

equation A-7 becomes, upon simplification:

$$\bar{v} = \frac{1}{p} \left\{ x' + \frac{1}{\sqrt{R_p}} \left[\sum_{m=0}^{\infty} e^{-\sqrt{R_p}(2m+2-x')} - \sum_{m=0}^{\infty} e^{-\sqrt{R_p}(2m+1-x')} - \sum_{m=0}^{\infty} e^{-\sqrt{R_p}(2m+1+x')} + \sum_{m=0}^{\infty} e^{-\sqrt{R_p}(2m+x')} \right] \right\} \quad (A-8)$$

Finding the inverse transform of each term in equation A-8 the solution for the velocity, strain and strain-rate are:

$$\bar{v}' = x' + 2\sqrt{\frac{t'}{R}} \left[\sum_{m=0}^{\infty} \text{ierfc} \left(\frac{2m+2-x'}{2\sqrt{\frac{t'}{R}}} \right) - \sum_{m=0}^{\infty} \text{ierfc} \left(\frac{2m+1-x'}{2\sqrt{\frac{t'}{R}}} \right) - \sum_{m=0}^{\infty} \text{ierfc} \left(\frac{2m+1+x'}{2\sqrt{\frac{t'}{R}}} \right) + \sum_{m=0}^{\infty} \text{ierfc} \left(\frac{2m+x'}{2\sqrt{\frac{t'}{R}}} \right) \right] \quad (A-9)$$

$$\epsilon = t' \left\{ 1 + 4 \left[\sum_{\eta=0}^{\infty} i^2 \operatorname{erfc} \left(\frac{2m+2-x'}{2\sqrt{\frac{t'}{R}}} \right) - \sum_{\eta=0}^{\infty} i^2 \operatorname{erfc} \left(\frac{2m+1-x'}{2\sqrt{\frac{t'}{R}}} \right) + \sum_{\eta=0}^{\infty} i^2 \operatorname{erfc} \left(\frac{2m+1+x'}{2\sqrt{\frac{t'}{R}}} \right) - \sum_{\eta=0}^{\infty} i^2 \operatorname{erfc} \left(\frac{2m+x'}{2\sqrt{\frac{t'}{R}}} \right) \right] \right\} \quad (\text{A-10})$$

$$\frac{\partial v'}{\partial x'} = 1 - \sum_{\eta=0}^{\infty} \operatorname{erfc} \left(\frac{2m+2-x'}{2\sqrt{\frac{t'}{R}}} \right) + \sum_{\eta=0}^{\infty} \operatorname{erfc} \left(\frac{2m+1-x'}{2\sqrt{\frac{t'}{R}}} \right) - \sum_{\eta=0}^{\infty} \operatorname{erfc} \left(\frac{2m+1+x'}{2\sqrt{\frac{t'}{R}}} \right) + \sum_{\eta=0}^{\infty} \operatorname{erfc} \left(\frac{2m+x'}{2\sqrt{\frac{t'}{R}}} \right) \quad (\text{A-11})$$

B. Constant Area Jet (Finite Difference Method)

The differential equation of motion is:

$$R \frac{\partial v'}{\partial t'} - \frac{\partial^2 v'}{\partial x'^2} = 0 \quad (9)$$

and the initial and boundary conditions are

$$v' = x' \quad \text{at } t' = 0 ; 0 \leq x' \leq 1$$

$$\frac{\partial v'}{\partial x'} = 0 \quad \text{at } t' > 0 ; x' = 0, x' = 1 \quad (10)$$

Cover the region of interest in the (x', t') plane with the mesh defined by

$$x'_i = iH, \quad t'_k = kL \quad \begin{matrix} i = 0, 1, 2, \dots \\ k = 0, 1, 2, \dots \end{matrix} \quad (\text{B-1})$$

Function values at mesh points will be characterized by appropriate subscripts; thus $v'_{i,k}$ will denote the value of the approximate solution $v'(x', t')$ at the mesh point $x = x_i$ and $t = t_k$. Replacing $\frac{\partial^2 v'}{\partial x'^2}$ by the central difference quotient and $\frac{\partial v'}{\partial t'}$

by the forward difference quotient in equation 9 yields

$$\frac{v'_{i+1,k} - 2v'_{i,k} + v'_{i-1,k}}{H^2} = R \frac{v'_{i,k+1} - v'_{i,k}}{L} \quad (\text{B-2})$$

The mesh width L in the time direction can be chosen so that the following stability criterion ¹² is satisfied,

$$L = \frac{H^2 R}{2} \quad (B-3)$$

By taking $L = .02$, H becomes $= .00589$. Substituting B-3 in B-2 gives

$$v'_{i,k+1} = \frac{1}{2} (v'_{i+1,k} + v'_{i-1,k}) \quad (B-4)$$

$v'_{i,k+1}$ is formed by taking the arithmetic mean of $v'_{i+1,k}$ and $v'_{i-1,k}$.

The boundary condition $\frac{\partial v'}{\partial x'} = 0$ at $\begin{cases} x = 0 \\ t > 0 \end{cases}$

can be handled in many different ways. ¹³ The following method was found to give best results.

Replace $\frac{\partial v'}{\partial x'}$ by the central difference quotient. In setting up the central difference quotient, functional values at exterior mesh points are needed. $\frac{\partial v'}{\partial x'} = 0$ is replaced by $\frac{(v'_{-1,k} - v'_{1,k}))}{2H} = 0$, which gives $v'_{-1,k} = v'_{1,k}$

Table 2 shows the values calculated by this method.

While calculating this Table, the initial value of v' corresponding to $x' = 0$ and $t' = 0$ is changed from 0 to .5H. This change was made with a view of obtaining an improvement in agreement with the boundary condition at $t' = 0$ and $x' = 0$.

C. Constant Area Jet - After Break-Up (Finite Difference Method)

The governing differential equation of motion is

$$R \frac{\partial v'}{\partial t'} - \frac{\partial^2 v'}{\partial x'^2} = 0$$

and the initial condition is: v' at $t' = 0$ and $.02 \leq x' \leq 1$ equal to v' at $t' = .24$ and $.02 \leq x' \leq 1$ from Appendix A.

Boundary condition:

$$\frac{\partial v'}{\partial x'} = 0 \text{ at } x' = .02 \text{ and } t' > 0$$

Proceeding in the same manner as in Appendix B, the partial differential equation is replaced by the following finite difference equation:

$$v'_{i,k+1} = \frac{1}{2} (v'_{i+1,k} + v'_{i-1,k}) \quad (C-1)$$

Values of v' at $t' = 0$ and $.02 \leq x' \leq 1$ are obtained from equation A-9

The boundary condition $\frac{\partial v'}{\partial x'} = 0$ at $\begin{cases} x' = .02 \\ t > 0 \end{cases}$ is handled in the same manner as in Appendix B.

~~Displacement u' for any x' and t' is calculated from the relation $u' = \int_0^{t'} v' dt$ by Simpson's rule. Strain $\epsilon = \frac{\partial u'}{\partial x'}$ is determined from the central difference formula, $\frac{u_{i+1,k} - u_{i-1,k}}{2H}$ for numerical differentiation.~~

D. Variable Area Jet (Finite Difference Method)

The governing differential equation is equation 14,

$$\frac{\partial^2 v'}{\partial x'^2} + \lambda \frac{\partial v'}{\partial x'} + B\lambda = R \frac{\partial v'}{\partial t'}$$

where $R^* \approx 1000$ $B \approx .72$, $\lambda = 2$

The initial and boundary conditions are:

$$\begin{aligned} v' &= x' \quad \text{at } t'=0 : x' \geq 0 \\ v' &= 0 \quad \text{at } x'=0 : t' \geq 0 \end{aligned} \quad (15)$$

Using the same notation as for constant area jet, and transforming the partial differential equation 14 into finite difference form, i.e.

replacing $\frac{\partial^2 v'}{\partial x'^2}$ and $\frac{\partial v'}{\partial x'}$ by the central difference quotients and $\frac{\partial v'}{\partial t'}$ by the forward difference

quotient, the following is obtained

$$\begin{aligned} & \frac{(v'_{i+1,k} - 2v'_{i,k} + v'_{i-1,k}))}{H^2} + \lambda \frac{(v'_{i+1,k} - v'_{i-1,k}))}{2H} + \\ & B\lambda = R \frac{v'_{i+1,k} - v'_{i,k}}{L} \end{aligned}$$

To satisfy the stability criterion put $\frac{RH^2}{L} = 2$

Taking $H = .004$ and $L = 8 \times 10^{-3}$, equation D-1 becomes

$$v'_{i,k+1} = .502 v'_{i+1,k} + .498 v'_{i-1,k} + 11.52 \times 10^{-6} \quad (D-2)$$

* The value R used previously is 1153. The present value of $R = 1000$ is used as a matter of convenience and to study the results qualitatively. However, $R = 1153$ will be used in the exact analysis.

Equation D-2 is obtained for the variable area jet.

If it is assumed that the area of cross-section of the jet increases in a certain region of x' and then remains constant, two finite difference equations for the problem are applicable, one for the region of variable area and one for the region of constant area. Equation D-2 is valid for the case of variable area. For the case of constant area $\lambda = 0$, therefore D-1 yields.

$$v'_{i, \kappa+1} = \left(\frac{v'_{i+1, \kappa} + v'_{i-1, \kappa}}{2} \right) \quad (D-3)$$

Table 4 shows values calculated from formulas D-2 and D-3. It is assumed that the area of the jet increases from $x = 0$ to $x' = .024$; and is constant for $x' > .024$

Displacement u' for any x' and t' are calculated from the relation $u' = \int_0^t v' dt$ by Simpson's rule. Strain

$\epsilon = \frac{\partial u'}{\partial x'}$ is calculated by using the central difference formula, $\frac{(u'_{i+1, \kappa} - u'_{i-1, \kappa})}{2H}$ for numerical differentiation. The values of $\frac{\partial v'}{\partial x'}$ and $\frac{\partial u'}{\partial x'}$ are plotted vs. x' in figures 6 and 7.

UNCLASSIFIED

UNCLASSIFIED